

SUPPORTING INFORMATION

Dissolution Kinetics of Hot Compressed Oxide Glasses

Nerea Mascaraque¹, Mathieu Bauchy², José Luis G. Fierro³, Sylwester J. Rzoska⁴, Michal Bockowski⁴, Morten M. Smedskjaer^{1,*}

¹*Department of Chemistry and Bioscience, Aalborg University, Aalborg 9220, Denmark*

²*Department of Civil and Environmental Engineering, University of California, Los Angeles, California 90095, USA*

³*Instituto de Catálisis y Petroleoquímica (CSIC), Cantoblanco, 28049 Madrid, Spain*

⁴*Institute of High-Pressure Physics, Polish Academy of Sciences, Warsaw, Poland*

* Corresponding author. E-mail: mos@bio.aau.dk

Figure S1. Deconvolution of O_{1s} core-level spectra of as-prepared and compressed P glasses. The dashed and solid lines represent the experimental and fitted data, respectively.

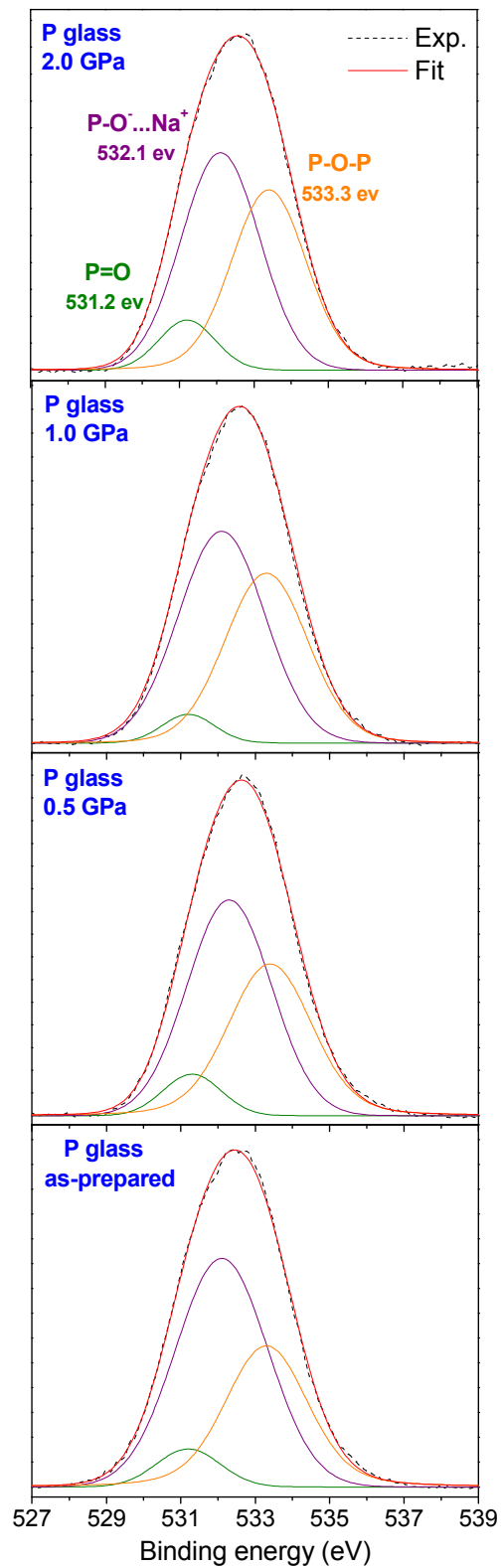


Figure S2. Deconvolution of O_{1s} core-level spectra of as-prepared and compressed BP glasses. The dashed and solid lines represent the experimental and fitted data, respectively.

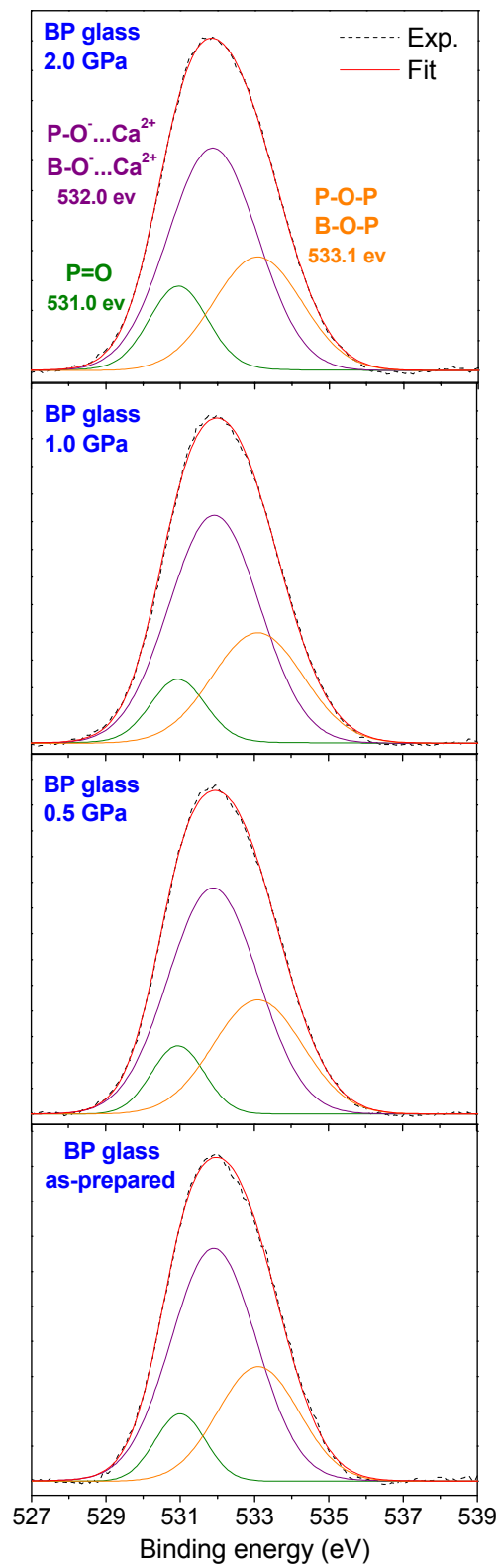


Figure S3. Deconvolution of O_{1s} core-level spectra of as-prepared and compressed BSi glasses. The dashed and solid lines represent the experimental and fitted data, respectively.

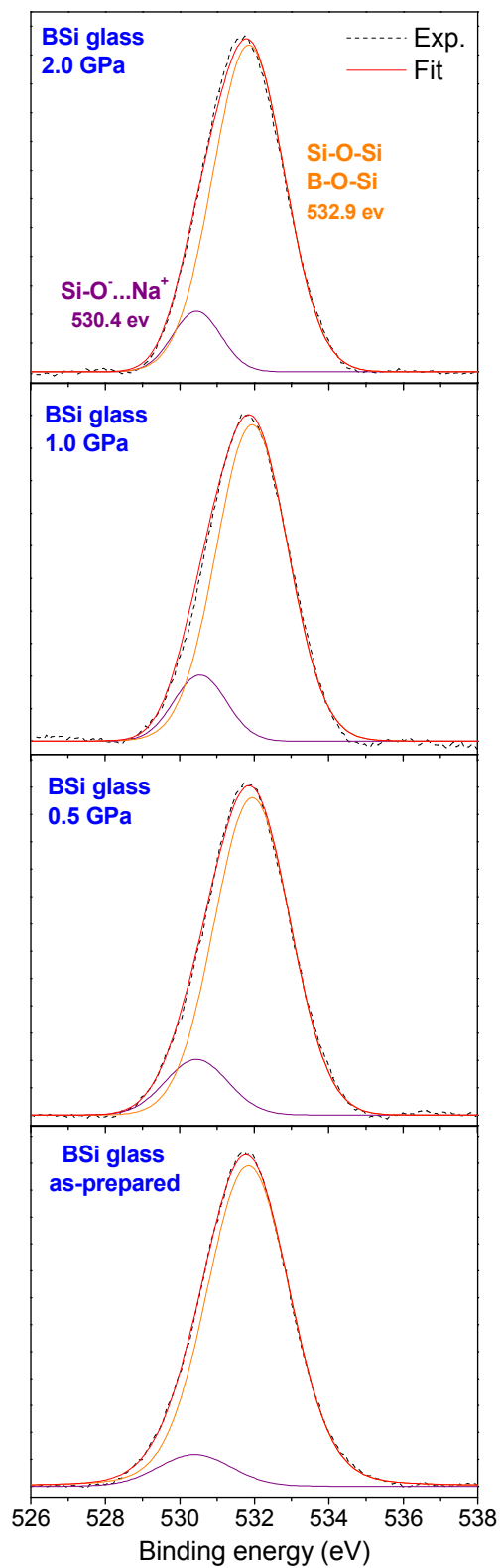


Figure S4. Deconvolution of O_{1s} core-level spectra of as-prepared and compressed AIBSi glasses. The dashed and solid lines represent the experimental and fitted data, respectively.

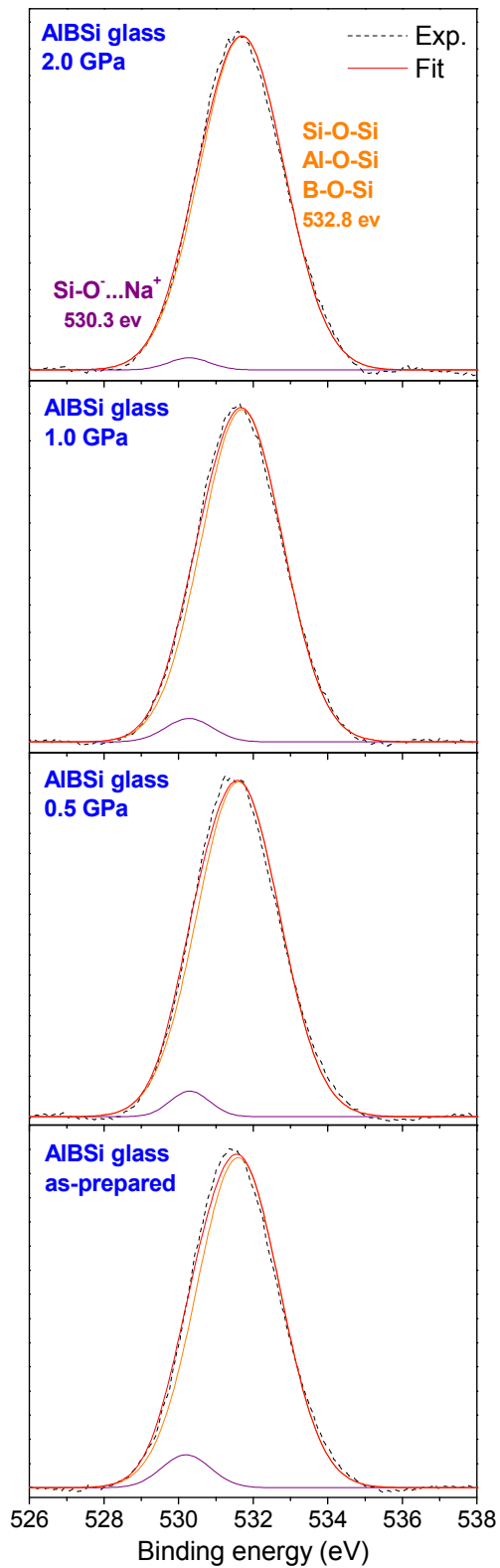


Figure S5. The hardness values obtained in this work (Table S1) as a function of the number of constraint per atom, n_c , obtained from Refs.³²⁻³⁵ The error in H_V is smaller than ± 0.12 GPa.

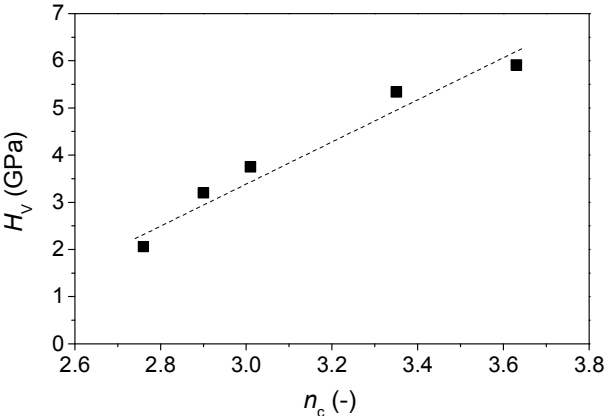


Figure S6. Weight loss (in mg dm^{-2}) of the densified P glass as a function of time (t in h) in different conditions: (a) pH=2 for $P=0.5$ GPa, (b) pH=7 for $P=0.5$ GPa, (c) pH=2 for $P=1.0$ GPa, (d) pH=7 for $P=1.0$ GPa, (e) pH=2 for $P=2.0$ GPa, and (f) pH=7 for $P=2.0$ GPa. Two repeated experiments are performed for each combination of glass, solution pH, and pressure. The dashed lines represent linear fits to the data.

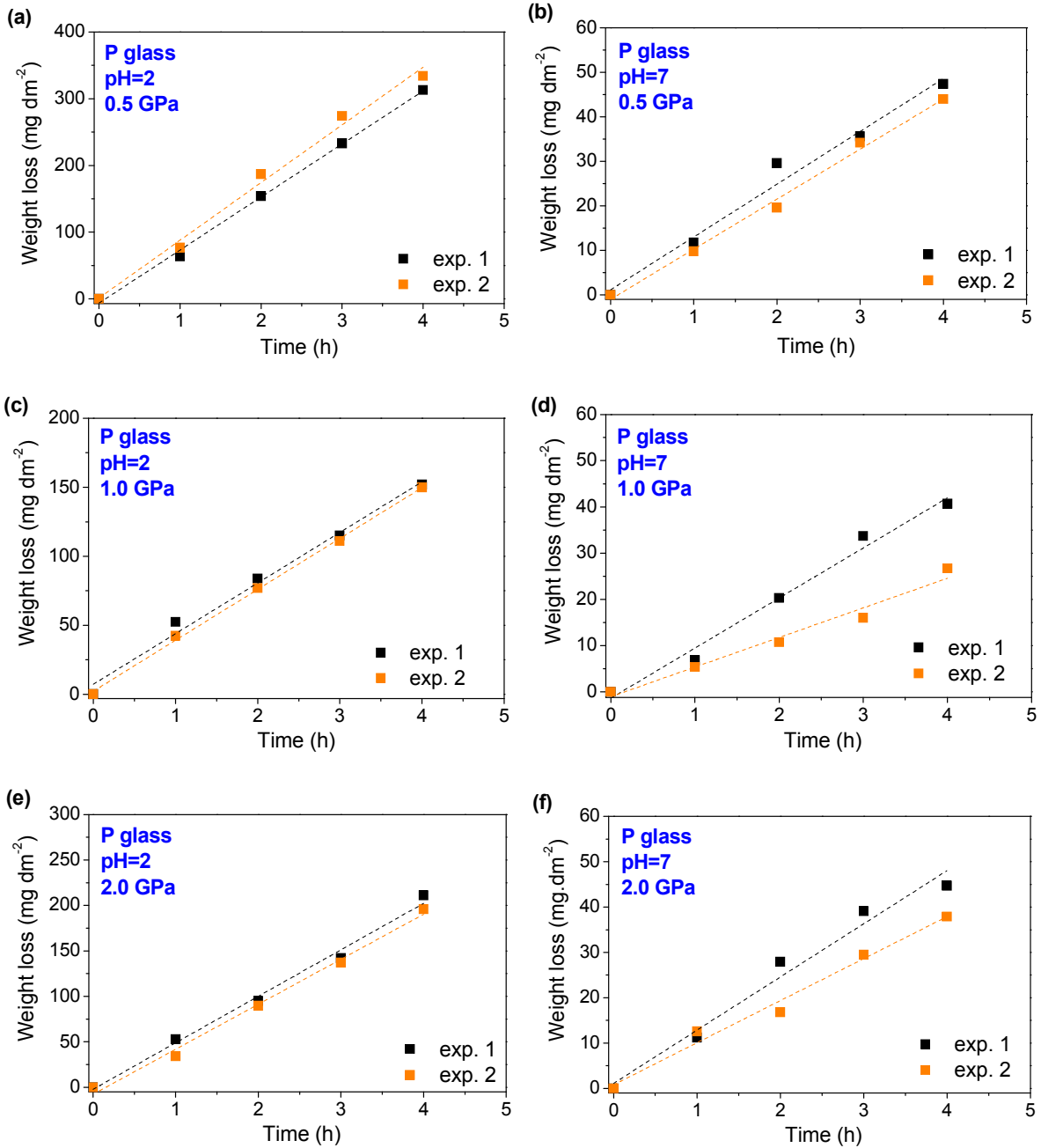


Figure S7. Weight loss (in mg dm^{-2}) of the densified BP glass as a function of time (t in h) in different conditions: (a) pH=2 for $P=0.5$ GPa, (b) pH=7 for $P=0.5$ GPa, (c) pH=2 for $P=1.0$ GPa, (d) pH=7 for $P=1.0$ GPa, (e) pH=2 for $P=2.0$ GPa, and (f) pH=7 for $P=2.0$ GPa. One experiment is performed for each combination of glass, solution pH, and pressure. Only one sample was analyzed as the second one had broken during the hot-compression process. The dashed lines represent linear fits to the data.

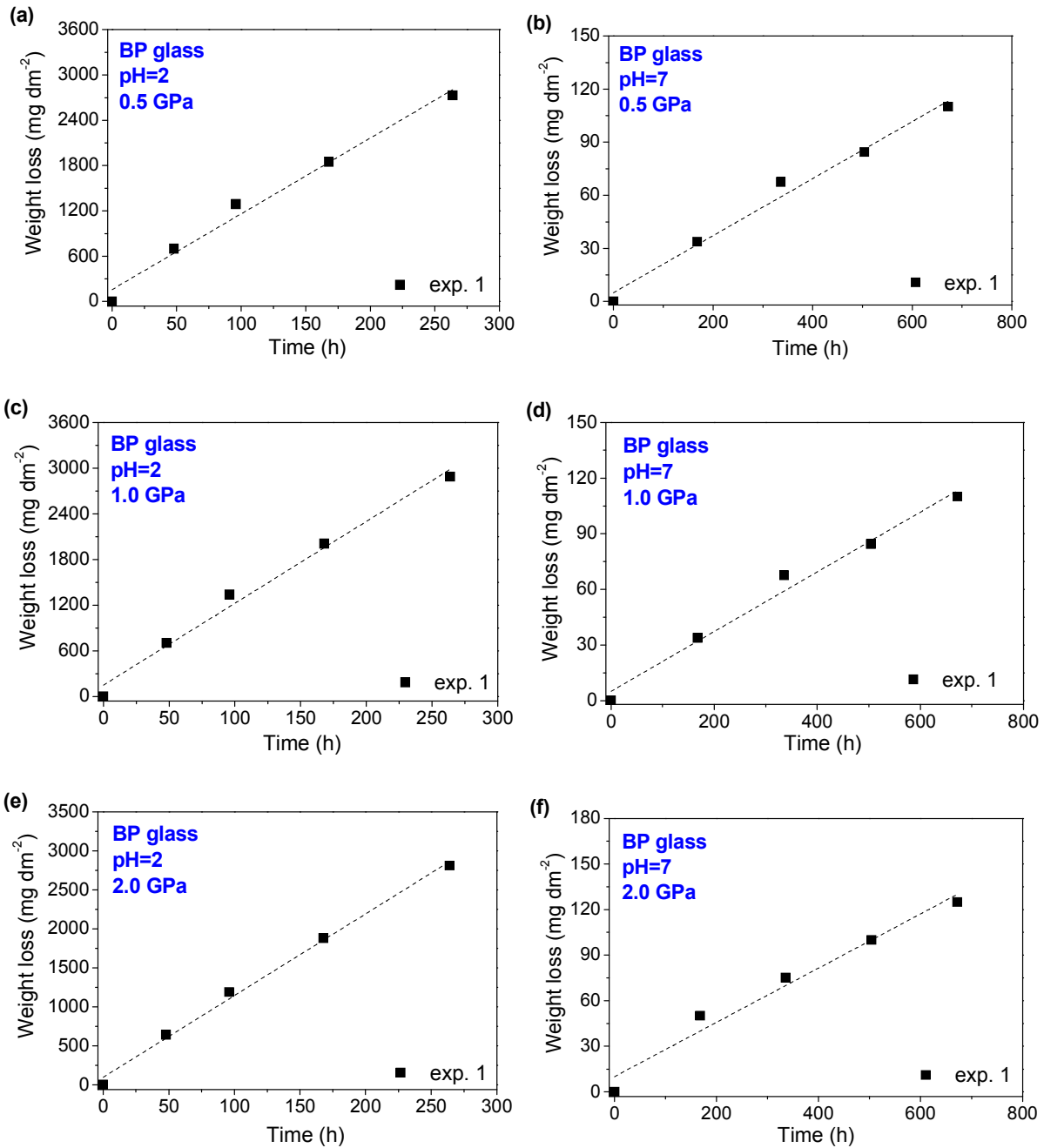


Figure S8. Weight loss (in mg dm^{-2}) of the densified BSi glass as a function of time (t in h) in different conditions: (a) pH=2 for $P=0.5$ GPa, (b) pH=7 for $P=0.5$ GPa, (c) pH=2 for $P=1.0$ GPa, (d) pH=7 for $P=1.0$ GPa, (e) pH=2 for $P=2.0$ GPa, and (f) pH=7 for $P=2.0$ GPa. Two repeated experiments are performed for each combination of glass, solution pH, and pressure. The dashed lines represent linear fits to the data.

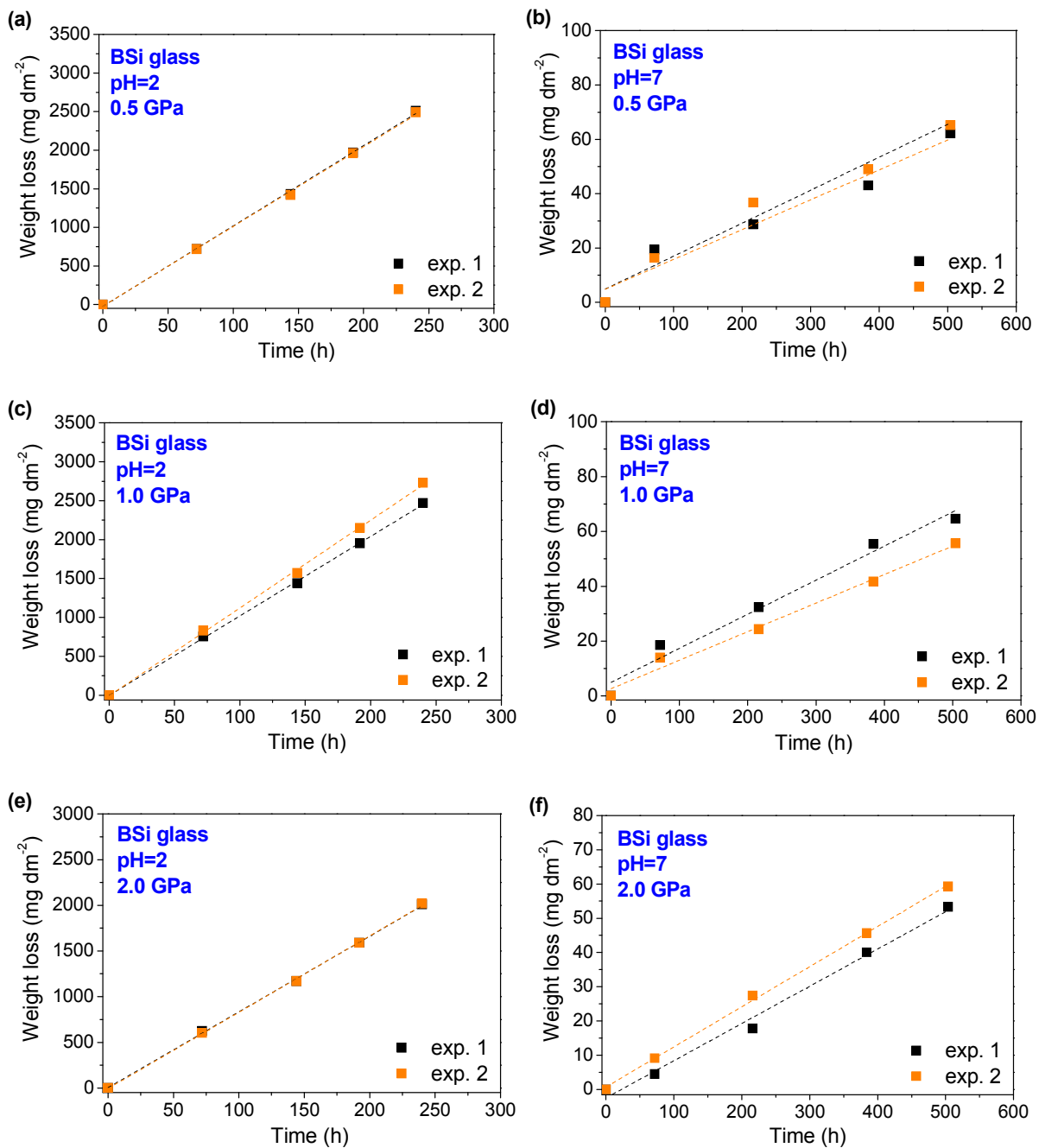


Figure S9. Weight loss (in mg dm^{-2}) of the densified AlBSi glass as a function of time (t in h) in different conditions: (a) pH=2 for $P=0.5$ GPa, (b) pH=7 for $P=0.5$ GPa, (c) pH=2 for $P=1.0$ GPa, (d) pH=7 for $P=1.0$ GPa, (e) pH=2 for $P=2.0$ GPa, and (f) pH=7 for $P=2.0$ GPa. Two repeated experiments are performed for each combination of glass, solution pH, and pressure. The dashed lines represent linear fits to the data.

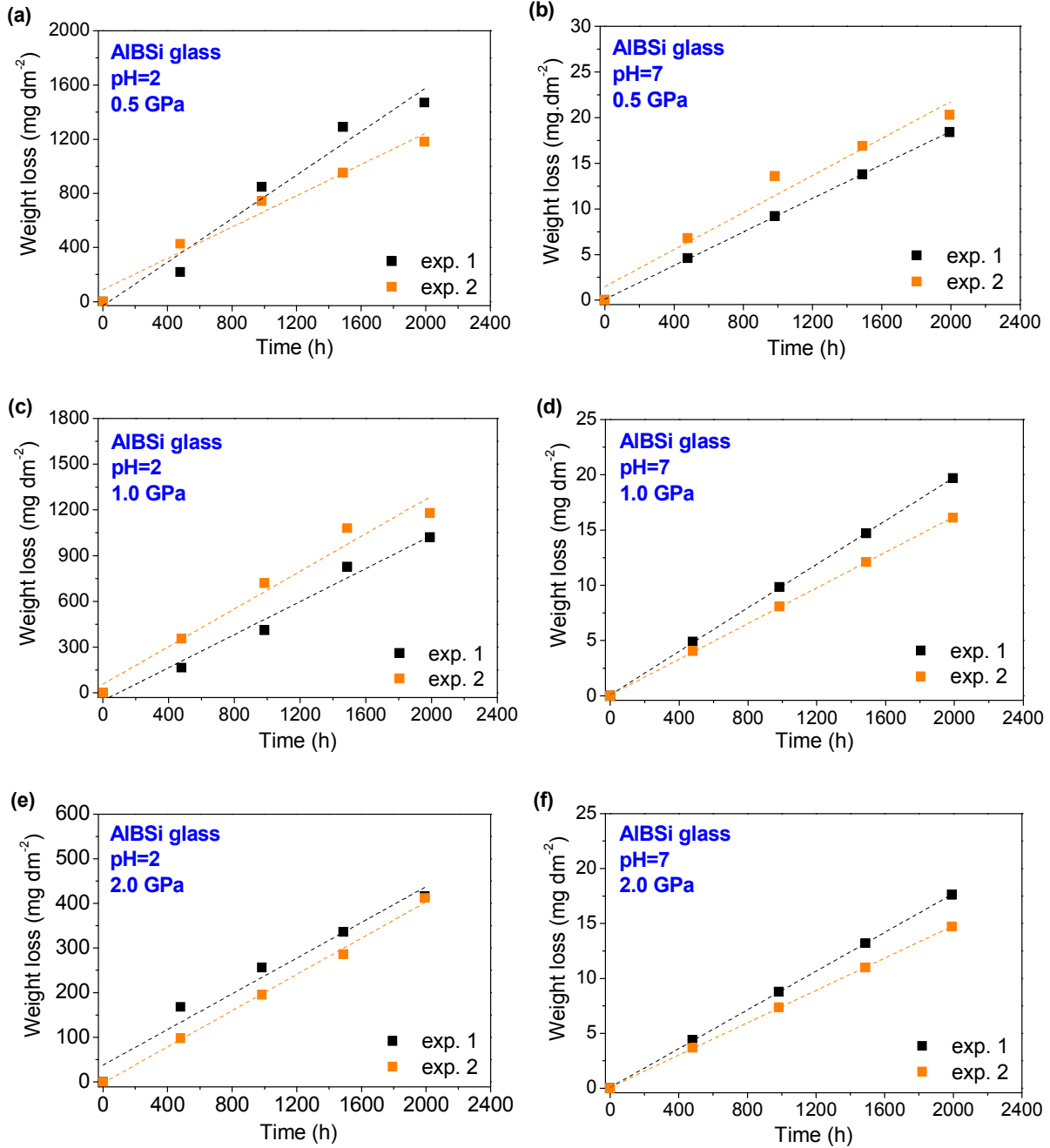


Figure S10. Pressure-induced change in the dissolution rate ($\Delta D_f/D_{f,0}$) as a function of the pressure-induced change in BO/NBO ratio ($\Delta\text{NBO}/\text{NBO}_0$) for (a) pH=2 and (b) pH=7.

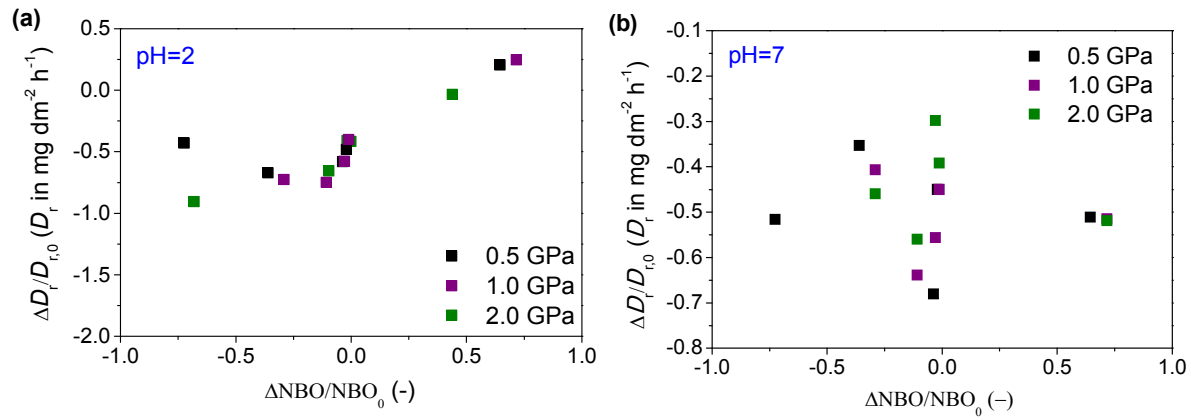


Figure S11. Concentration of leached Na^+ ions as a function of immersion time for dissolution of (a) P glass and (b) SiP glass at both pH = 2 and pH = 7. The calculated concentrations of Na^+ are by assuming congruent dissolution. We observe linear increase in Na^+ leaching concentration with time for both pH values, with measured values being close to the calculated ones, i.e., we observe congruent leaching of the modifier. As such, the leaching studies performed in P and SiP glasses suggest a congruency in the diffusion of Na^+ modifier for each immersion time and pH values.

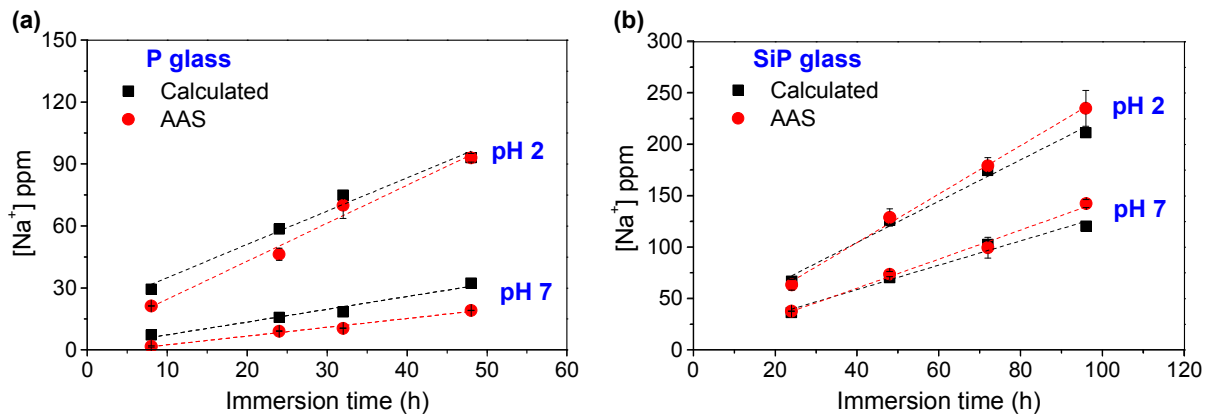


Figure S12. Pressure-induced change in the dissolution rate ($\Delta D_r/D_{r,0}$) as a function of the pressure-induced change in density ($\Delta\rho/\rho_0$) for (a) pH=2 and (b) pH=7.

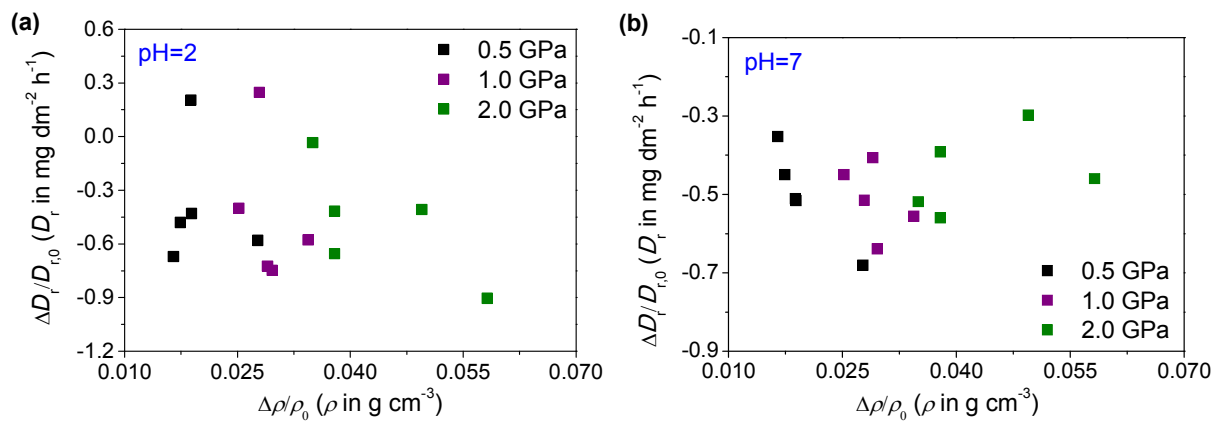


Figure S13. Dependence of the natural logarithm of the dissolution rate (D_r , in $\text{mg dm}^{-2} \text{h}^{-1}$) in different aqueous solutions (pH = 2 and 7) on the number of atomic constraints per atom (n_c) of the as-prepared and densified oxide glasses (0-2.0 GPa). The data for the as-prepared glasses are taken from Refs.³²⁻³⁵ Lines represent linear fits to the data.

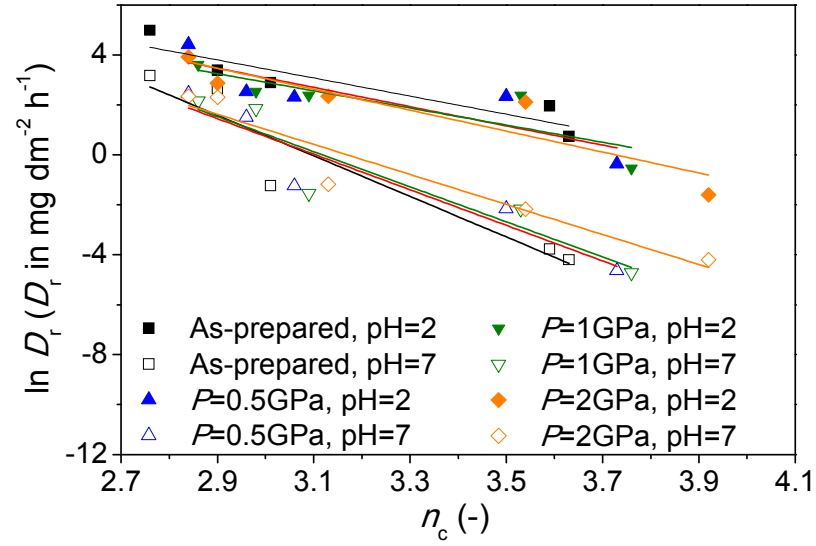


Table S1. Density (ρ) and Vickers hardness (H_V) values of all the as-prepared and compressed oxide glasses at 0.5, 1.0, and 2.0 GPa. The errors associated with ρ and H_V are within $\pm 0.002 \text{ g cm}^{-3}$ and $\pm 0.18 \text{ GPa}$, respectively.

ID	As-prepared		Compressed at 0.5 GPa		Compressed at 1.0 GPa		Compressed at 2.0 GPa	
	ρ (g cm^{-3})	H_V (GPa)	ρ (g cm^{-3})	H_V (GPa)	ρ (g cm^{-3})	H_V (GPa)	ρ (g cm^{-3})	H_V (GPa)
P	2.430	2.06	2.476	2.41	2.502	2.51	2.522	2.42
SiP	2.520	3.20	2.590	3.46	2.610	3.54	2.645	3.21
BP	2.682	3.75	2.729	3.95	2.750	4.12	2.784	4.27
BSi	2.540	5.34	2.588	5.99	2.611	6.15	2.629	6.18
AlBSi	2.396	5.91	2.436	6.34	2.466	6.47	2.536	7.19

Table S2. Concentration of sodium and calcium (in ppm) in the pH=2 (acid media) and pH=7 (neutral media) solutions following dissolution experiments of the glasses. The concentrations are measured after the end of bulk dissolution testing, i.e., after the last immersion time, using AAS spectrometer, and the calculated concentrations are obtained from the weight loss at the end of the experiment and the initial molar composition of each oxide glass. A higher concentration of sodium or calcium is measured in the pH = 2 solution compared to that in pH = 7, implying that the rate of the diffusion process is faster for lower pH. For the flexible densified glasses (P and SiP), the calculated and measured concentration values are fairly similar, indicating that the dissolution of modifier is congruent. In the densified BP glasses, the measured Ca^{2+} concentration in acidic and neutral media is lower than the calculated values, confirming that the diffusion of Ca^{2+} across the glass is slower than for Na^+ , and consequently that the modifier dissolution is not congruent. In the densified BSi glasses which contain both Ca^{2+} and Na^+ , a clear difference in the rate of diffusion between Ca^{2+} and Na^+ is observed. While the calculated and measured $[\text{Na}^+]$ values are fairly similar for pH= 2 and 7, the measured $[\text{Ca}^{2+}]$ is lower for neutral media and similar in acid solutions. This indicates that the degree of congruency of modifier dissolution in glass systems with different cations depends on the pH. In stressed-rigid densified AIBSi glasses, the leaching rate of Na^+ depends on the pressure, and the degree of congruency in the modifier dissolution increases with increasing pressure.

Glass ID	[Na ⁺] in ppm				[Ca ²⁺] in ppm			
	pH=2 (calc.)	pH=2 (AAS)	pH=7 (calc.)	pH=7 (AAS)	pH=2 (calc.)	pH=2 (AAS)	pH=7 (calc.)	pH=7 (AAS)
P-0.5	17.2	10.0 ± 0.1	2.6	2.6 ± 0.1	n/a	n/a	n/a	n/a
P-1.0	11.4	8.70 ± 0.9	1.7	2.01 ± 0.1	n/a	n/a	n/a	n/a
P-2.0	13.4	13.4 ± 0.3	2.6	2.1 ± 0.1	n/a	n/a	n/a	n/a
SiP-0.5	45.7	45.8 ± 2.7	16.8	18.2 ± 0.9	n/a	n/a	n/a	n/a
SiP-1.0	44.5	43.4 ± 1.8	16.8	16.2 ± 0.5	n/a	n/a	n/a	n/a
SiP-2.0	103.4	108.7 ± 2.0	42.6	37.1 ± 0.9	n/a	n/a	n/a	n/a
BP-0.5	n/a	n/a	n/a	n/a	146.2	61.2 ± 0.3	4.2	2.5 ± 0.1
BP-1.0	n/a	n/a	n/a	n/a	179.0	80.6 ± 1.9	5.5	3.5 ± 0.1
BP-2.0	n/a	n/a	n/a	n/a	136.1	73.6 ± 3.7	4.2	2.5 ± 0.1
BSi-0.5	114.5	109.8 ± 1.1	2.9	4.2 ± 0.1	66.6	61.6 ± 0.4	1.7	0.4 ± 0.1
BSi-1.0	107.7	107.7 ± 1.3	3.6	4.7 ± 0.1	62.7	58.1 ± 0.1	2.1	0.7 ± 0.1
BSi-2.0	97.4	91.3 ± 3.6	2.7	3.2 ± 0.2	56.7	54.9 ± 0.1	1.6	0
AIBSi-0.5	36.9	13.1 ± 0.7	0.2	0.2 ± 0.1	n/a	n/a	n/a	n/a
AIBSi-1.0	31.4	12.8 ± 2.3	0.2	0.1 ± 0.1	n/a	n/a	n/a	n/a
AIBSi-2.0	12.0	11.5 ± 0.9	0.2	0.2 ± 0.1	n/a	n/a	n/a	n/a